

Truncated Perfect Actions for Staggered Fermions

W. Bietenholz ^a and H. Dilger ^b

^a HLRZ c/o Forschungszentrum Jülich
D-52425 Jülich, Germany

^b Institute for Theoretical Physics I
WWU Münster
Wilhelm-Klemm Str. 9
D-48149 Münster, Germany

Preprint HLRZ 1998-10

We discuss the behavior of free perfect staggered fermions and truncated versions thereof. The study includes flavor non-degenerate masses. We suggest a new blocking scheme, which provides excellent locality of the perfect lattice action. A truncation procedure adequate for the structure of staggered fermions is applied. We consider spectral and thermodynamic properties and compare truncated perfect actions, Symanzik improved and standard staggered fermions in two and four dimensions.

1 Introduction

The inclusion of dynamical fermions in simulations of gauge theories, in particular QCD, is a major issue in lattice field theory. Such simulations have generally been performed either using Wilson fermions [1] or staggered fermions [2]. The latter formulation is especially useful in the chiral limit, because the remnant chiral symmetry $U(1) \otimes U(1)$ protects the zero fermion mass from renormalization. As a related virtue, its artifacts due to the lattice spacing a are only of $O(a^2)$, whereas they are of $O(a)$ for Wilson fermions interacting by gauge fields.

It is now widely accepted that the above lattice actions should be improved, so that the lattice spacing artifacts are suppressed and coarser lattices can be used, particularly in QCD simulations [3]. There are essentially two improvement strategies in the literature. In Symanzik's program [4] the action is improved order by order in a . For QCD with Wilson fermions this has been realized on-shell to the first order on the classical level [5] and recently also on the quantum level [6]. Less work has been devoted to the improvement of staggered fermions, perhaps because the artifacts in the standard formulation are already smaller. However, S. Naik has applied Symanzik's program on-shell, where he improved the free staggered fermion by adding more couplings along the axes [7], and the Bielefeld group did the same by adding diagonal couplings [8]. Furthermore, the MILC collaboration achieved a reduced pion mass by treating the gauge variable as a "fat link" [9]. Finally, some work on improved operators has been done in this framework [10].

The other promising improvement scheme is non-perturbative in a and uses renormalization group concepts. It has been known for a long time that there are perfect lattice actions in the parameter space, i.e. actions without any lattice artifacts [11]. Recently it has been suggested to approximate them for asymptotically free theories as "classically perfect actions" [12], which works very well in a number of two dimensional models [12, 13, 14].

For free or perturbatively interacting fields, perfect actions can be constructed analytically in momentum space. For Wilson type fermions this has been carried out to the first order in the gauge coupling in the Schwinger model [15] and in QCD [16]. A technique called "blocking from the continuum" was extremely useful for this purpose. One expresses all quantities in lattice units after the blocking, and sends the blocking factor to infinity. Hence the blocking process starts from a continuum theory, and it does not need to be iterated in order to identify a perfect action.

For staggered fermions a block variable renormalization group transformation (RGT), which does not mix the pseudo flavors and which does therefore preserve the important symmetries, has been suggested in Ref. [17]. It requires an odd blocking factor n . Iterating the $n = 3$ block variable RGT, a fixed point action, i.e. a perfect action at infinite correlation length, has been constructed [13, 18]. Also for staggered fermions blocking from the continuum is applicable [19]. This has been carried out for a general (flavor non-degenerate) mass term, revealing the intimate relation to the Dirac-Kähler fermion

formulation in the continuum [20], and also including a suitable treatment of the gauge field [21]. Using the generalization to a flavor non-degenerate mass, the spectral doublers inherent to the staggered fermion formulation might be treated as physical flavors in a QCD simulation.

For any blocking scheme, the perfect action displays the continuum scaling behavior by definition. In practice, however, the approximations in the determination of an applicable quasi perfect action violate this property to some extent. With this respect, the choice of the RGT is very important.

In the present paper, we first review the procedure of blocking staggered fermions from the continuum, adding new aspects. We then discuss the optimization of locality, in the sense of an extremely fast exponential decay of the couplings in coordinate space. This property is crucial for practical applications, because we have to truncate the couplings to a small number, which is manageable in simulations. For excellent locality, the violation of perfectness due to truncation is not too harmful. Moreover, the virtues of staggered fermions come into play: the truncation induces errors of $O(a^2)$ at most, and the remnant axial symmetry is preserved in the truncated perfect action, hence it still excludes additive mass renormalization. On the other hand, a strong mass renormalization is a severe problem for truncated perfect fermions of the Wilson type [22, 23].

We suggest a new blocking scheme, which leads to a higher degree of locality than the usual block average method. Still the couplings decay exponentially in coordinate space. We then truncate them to a short range by means of mixed periodic and antiperiodic boundary conditions, which are particularly suitable for staggered fermions. We finally compare the spectra and the scaling of thermodynamic quantities for several truncated perfect, Symanzik improved and standard staggered fermions. The discussion of the spectrum includes also the case of non-degenerate masses of the pseudo flavors. It turns out that the new blocking scheme, which we call “partial decimation”, does consistently yield excellent results. Moreover, for that scheme, optimal locality is reached by the simple δ function RGT in the massless case, in contrast to the block average scheme.

Simulation results for the Schwinger model based on this action will be presented in a subsequent paper [24].

2 The Staggered Blocking Scheme

The construction of perfect actions for free staggered fermions by blocking from the continuum has been described in Refs. [20, 21]. Let us briefly review this procedure. The staggered blockspin fermions are defined in two steps. First we transform the $N_f = 2^{d/2}$ flavors of continuum Dirac spinors $\psi_a^b(x)$ (a : spinor index, b : flavor index) into the Dirac-Kähler (DK) representation by $\varphi(x, H)$.¹ These functions are considered as component

¹For the relation of the DK formulation of continuum fermions [25] with staggered lattice fermions we refer to Ref. [26]. A relation to the present block spin transformation is discussed in Ref. [20].

functions of inhomogeneous differential forms

$$\Phi = \sum_H \varphi(x, H) dx^H, \quad dx^H = dx^{\mu_1} \wedge \dots \wedge dx^{\mu_h}, \quad (2.1)$$

where $H = \{\mu_1, \dots, \mu_h\}$, $\mu_1 < \dots < \mu_h$ is a multi-index. Transformation and inverse transformation read

$$\varphi(x, H) = \frac{1}{\sqrt{N_f}} \sum_{ab} \gamma_{ab}^{H*} \psi_a^b(x), \quad \gamma^H = \gamma^{\mu_1} \gamma^{\mu_2} \dots \gamma^{\mu_h}, \quad (2.2)$$

$$\psi_a^b(x) = \frac{1}{\sqrt{N_f}} \sum_H \gamma_{ab}^H \varphi(x, H). \quad (2.3)$$

Second, we introduce a coarse lattice of unit spacing $\bar{\Gamma} = \{\bar{y} | \bar{y}_\mu = \bar{n}_\mu\}$, which is a sublattice of $\Gamma = \{y | y_\mu = n_\mu/2\}$, with $\bar{n}_\mu, n_\mu \in \mathbb{Z}$. The fine lattice points y are uniquely decomposed as ($\hat{\mu}$ is the unit vector in μ -direction)

$$y = \bar{y} + e_H/2, \quad e_H = \sum_{\mu \in H} \hat{\mu}. \quad (2.4)$$

Thus the multi-index $H(y)$ defines the position of a fine lattice point y with respect to the coarse lattice $\bar{\Gamma}$. Now the blockspin variables $\phi(y)$ can be defined as averages of the component functions $\varphi(x, H(y))$, with a normalized weight $\Pi(x-y)$, $\int dx \Pi(x-y) = 1$, which is assumed to be even and peaked around $x = y$,

$$\phi(y) = \frac{1}{\sqrt{N_f}} \sum_{ab} \gamma_{ab}^{H(y)*} \int dx \Pi(x-y) \psi_a^b(x). \quad (2.5)$$

This scheme has been proposed first in Ref. [19]. Its peculiarity is that the staggered block centers depend on the multi-index H of the Dirac-Kähler component functions $\varphi(x, H)$. Block average (BA) means in this case average over the overlapping lattice hypercubes $[y] = \{x | -1/2 \leq (x_\mu - y_\mu) \leq 1/2\}$. This scheme is given by $\Pi = \Pi_{BA}$, $\Pi_{BA}(x) = 1$ for $x \in [y]$, $\Pi_{BA}(x) = 0$ otherwise.

For the following calculation we diagonalize the lattice action using the staggered symmetries. Here it is important that fine lattice shifts are no symmetry transformations. However, combination with site-dependent sign factors gives rise to the non-commuting flavor symmetry transformations [27]. Therefore we replace ordinary Fourier transformation by harmonic analysis with respect to flavor transformations and coarse lattice translations. We thus obtain a modified momentum representation which intertwines Fourier transformation and the transition back from DK fermions to the Dirac basis,

$$\begin{aligned} \phi_a^b(p) &= \sum_y e^{ipy} \gamma_{ab}^{H(y)*} \phi(y), \\ \bar{\phi}_a^b(p) &= \sum_y e^{ipy} \gamma_{ab}^{H(y)} \bar{\phi}(y), \quad p \in \mathcal{B} =]-\pi, \pi]^d. \end{aligned} \quad (2.6)$$

Inserting Eq. (2.5) we find

$$\phi_a^b(p) = \frac{1}{\sqrt{N_f}} \int \frac{dp'}{(2\pi)^d} \sum_{a'b'} \Pi(p') \psi_{a'}^{b'}(p') \sum_y e^{i(p-p')y} \gamma_{ab}^{H(y)} \gamma_{a'b'}^{H(y)*}, \quad (2.7)$$

where $\psi_a^b(p), \Pi(p)$ denote the Fourier transform of $\psi_a^b(x), \Pi(x)$. The last sum can be re-written as

$$\begin{aligned} \sum_{\bar{y} \in \bar{\Gamma}} e^{iq\bar{y}} \sum_K e^{iqe\kappa/2} \gamma_{ab}^K \gamma_{a'b'}^{K*} &= (2\pi)^d \sum_{l \in \mathbb{Z}^d} \delta(q - 2\pi l) \sum_K \prod_{\mu \in K} (-1)^{l_\mu} \gamma_{ab}^K \gamma_{a'b'}^{K*} \\ &= N_f (2\pi)^d \sum_{l \in \mathbb{Z}^d} \delta(q - 2\pi l) \gamma_{aa'}^{\hat{H}(l)} \gamma_{b'b}^{\hat{H}(l)\dagger}. \end{aligned} \quad (2.8)$$

We have used the orthogonality of the γ -matrix elements

$$\sum_H \gamma_{ab}^H \gamma_{a'b'}^{H*} = N_f \delta_{aa'} \delta_{bb'}, \quad (2.9)$$

and $\hat{H}(l)$ is defined by $H(l) = \{\mu | l_\mu \text{ is odd}\}$, $\hat{H} = H$ for h even, $\hat{H} = \{\mu | \mu \notin H\}$ for h odd. Finally Eq. (2.7) becomes (summation over double spin and flavor indices is understood)

$$\phi_a^b(p) = \sqrt{N_f} \sum_{l \in \mathbb{Z}^d} \Pi(p+2\pi l) \hat{\psi}_{a'}^{b'}(p+2\pi l), \quad \hat{\psi}_a^b(p+2\pi l) = \gamma_{aa'}^{\hat{H}(l)} \psi_{a'}^{b'}(p+2\pi l) \gamma_{b'b}^{\hat{H}(l)\dagger}. \quad (2.10)$$

Note that the blockspin transformation is diagonal with respect to spin and flavor for continuum momenta within the first Brillouin zone \mathcal{B} , yet not for all $l \neq 0$.

We are now prepared to compute the perfect action for a RGT of the Gaussian type. Starting from a continuum action with a general mass term m_b – which does not need to be flavor degenerate – the perfect lattice action $S[\bar{\phi}, \phi]$ is defined as

$$\begin{aligned} e^{-S[\bar{\phi}, \phi]} &= \int \mathcal{D}\bar{\psi} \mathcal{D}\psi \int \mathcal{D}\bar{\eta} \mathcal{D}\eta \exp\left\{-\int \frac{dq}{N_f(2\pi)^d} \bar{\psi}_a^b(-q) (i\gamma_{aa'}^\mu q_\mu + m_b) \psi_{a'}^b(q)\right\} \\ &\times \exp\left\{\int_{\mathcal{B}} \frac{dp}{N_f(2\pi)^d} \left[[\bar{\phi}_a^b(-p) - \sqrt{N_f} \sum_{l \in \mathbb{Z}^d} \Pi(p+2\pi l) \hat{\psi}_a^b(-p-2\pi l)] \eta_a^b(p) \right. \right. \\ &\quad \left. \left. + \bar{\eta}_a^b(-p) [\phi_a^b(p) - \sqrt{N_f} \sum_{l \in \mathbb{Z}^d} \Pi(p+2\pi l) \hat{\psi}_a^b(p+2\pi l)] \right. \right. \\ &\quad \left. \left. + \bar{\eta}_a^b(-p) D_{aa'}^b(p) \eta_{a'}^b(p) \right] \right\} \end{aligned} \quad (2.11)$$

A non-zero term

$$D_{aa'}^b(p) = \gamma_{aa'}^\mu D_\mu^b(p) + \delta_{aa'} D_0^b(p) \quad (2.12)$$

“smears out” the blockspin transformation, as in Ref. [21]. This term is used to optimize locality of the resulting perfect action; it will be specified later on. The Gaussian integrals over $\psi, \bar{\psi}$ and $\bar{\eta}, \eta$ can be evaluated by substitution of the classical fields leading to ²

$$S[\bar{\phi}, \phi] = \int_{\mathcal{B}} \frac{dp}{N_f (2\pi)^d} \left[\bar{\phi}_a^b(-p) G^{-1bb'}(p) \phi_{a'}^{b'}(p) \right], \quad (2.13)$$

with the lattice propagator

$$G_{aa'}^{bb'}(p) = D_{aa'}^{bb'}(p) + \sum_{l \in \mathbb{Z}^d} \left(\Pi(p+2\pi l)^2 \gamma_{bd}^{\hat{H}(l)} \frac{[-i(-1)^{k\nu} \gamma_{aa'}^\mu (p+2\pi l)_\mu + m_d] \delta_{dd'}}{(p+2\pi l)^2 + m_d^2} \gamma_{d'b'}^{\hat{H}(l)\dagger} \right). \quad (2.14)$$

Note that G is flavor diagonal, $G^{bb'} = G^b \delta^{bb'}$, because $\gamma^{\hat{H}(l)} \gamma^K \gamma^{\hat{H}(l)\dagger}$ is diagonal iff γ^K is. In particular, for a degenerate mass term the adjunction with $\gamma^{\hat{H}(l)}$ is trivial, and the lattice propagator is proportional to $\delta_{bb'}$ in flavor space. We define

$$G_{aa'}^b(p) = -i \sum_{\mu} \gamma_{aa'}^\mu Q_\mu^b(p) + \delta_{aa'} Q_0^b(p), \quad (2.15)$$

hence Q_μ^b, Q_0^b become

$$Q_\mu^b(p) = D_\mu^b(p) + \sum_{l \in \mathbb{Z}^d} \Pi(p+2\pi l)^2 \frac{1}{N_f} \sum_{b'} \sum_K \epsilon_K(l) \gamma_{bb}^K \gamma_{b'b'}^{K*} \frac{(-1)^{l_\mu} (p+2\pi l)_\mu}{(p+2\pi l)^2 + m_{b'}^2}, \quad (2.16)$$

$$Q_0^b(p) = D_0^b(p) + \sum_{l \in \mathbb{Z}^d} \Pi(p+2\pi l)^2 \frac{1}{N_f} \sum_{b'} \sum_K \epsilon_K(l) \gamma_{bb}^K \gamma_{b'b'}^{K*} \frac{m_{b'}}{(p+2\pi l)^2 + m_{b'}^2}. \quad (2.17)$$

In case of a non-degenerate mass m_b the sums $\sum_{b'} \sum_K$ can not be contracted according to Eq. (2.9), due to the sign factor $\epsilon_K(l) = \prod_{\nu \in K} (-1)^{l_\nu}$. However, in the degenerate case $m_b = m$, with flavor independent smearing terms $D^b = D$, we simply obtain

$$Q_\mu(p) = D_\mu(p) + \sum_{l \in \mathbb{Z}^d} \Pi(p+2\pi l)^2 \frac{(-1)^{l_\mu} (p+2\pi l)_\mu}{(p+2\pi l)^2 + m^2}, \quad (2.18)$$

$$Q_0(p) = D_0(p) + \sum_{l \in \mathbb{Z}^d} \Pi(p+2\pi l)^2 \frac{m}{(p+2\pi l)^2 + m^2}. \quad (2.19)$$

The perfect action in real space arises from Eq. (2.13) inserting the momentum representation Eq. (2.6). After some γ -matrix algebra [20], we arrive at

$$S[\bar{\phi}, \phi] = \sum_{y, y'} \bar{\phi}(y) m(y, y') \phi(y'), \quad (2.20)$$

$$m(y, y') = \sum_K \rho^K(y') \rho(y - y', y') M^K(y - y'). \quad (2.21)$$

²We ignore constant factors in the partition function.

Corresponding to a lattice propagator diagonal in flavor space, the sum over K runs over multi-indices $K \in \mathcal{D}$ with diagonal γ^K , in the Weyl basis $\mathcal{D} = \{\emptyset, 12, 34, 1234\}$. The sign factors $\rho(z, y) \equiv \rho(H(z), H(y))$ arise from $\gamma^H \gamma^K = \rho(H, K) \gamma^{H\Delta K}$, where $H\Delta K = (H \cup K) \setminus (H \cap K)$, and $\rho^K(y)$ is given by $\rho(H(y), K) \rho(K, H(y))$. By symmetry, the only non-zero contributions to $M^K(y)$ are

$$M_\mu^K(y) = i\rho(\mu, K) \int_{\mathcal{B}} \frac{dp}{(2\pi)^d} e^{-ipy} M_\mu^K(p) \quad \text{for } H(y) = \mu\Delta K, \quad (2.22)$$

$$M_0^K(y) = \int_{\mathcal{B}} \frac{dp}{(2\pi)^d} e^{-ipy} M_0^K(p) \quad \text{for } H(y) = K, \quad (2.23)$$

$$\text{with } M_{\mu,0}^K(p) = \frac{1}{N_f} \sum_b \gamma_{bb}^{K*} \frac{Q_{\mu,0}^b(p)}{\sum_\mu Q_\mu^b(p)^2 + Q_0^b(p)^2}. \quad (2.24)$$

The flavor degenerate case leads to vanishing components for $K \neq \emptyset$, and for $M_{\mu,0}^\emptyset \equiv M_{\mu,0}$ we simply obtain

$$M_{\mu,0}(p) = \frac{Q_{\mu,0}(p)}{\sum_\nu Q_\nu(p)^2 + Q_0(p)^2}. \quad (2.25)$$

It has been proven in Ref. [20] that the couplings given by the fermion matrix $m(y, y')$ are local, i.e. they decay faster than any power of $|y - y'|$. For that, certain periodicity properties apply, which translate into (for simplicity of notion let $\tilde{\mu}$ denote either μ or 0, $K\Delta 0 \equiv K$)

$$Q_{\tilde{\mu}}^b(p) = \sum_{K \in \mathcal{D}} \gamma_{bb}^K Q_{\tilde{\mu}}^K(p), \quad Q_{\tilde{\mu}}^K(p + 2\pi\hat{\nu}) = \begin{cases} -Q_{\tilde{\mu}}^K(p) & \text{for } \nu \in K\Delta\tilde{\mu} \\ Q_{\tilde{\mu}}^K(p) & \text{for } \nu \notin K\Delta\tilde{\mu} \end{cases}. \quad (2.26)$$

Again, we sum over diagonal γ -matrices only. It is provided that the corresponding requirements are met for the smearing terms $D_{\tilde{\mu}(p)}^b$ within $Q_{\tilde{\mu}}^b(p)$, see below. In consequence, the fermion matrix components $M_{\tilde{\mu}}^K(p)$ obey periodicity conditions analogous to $Q_{\tilde{\mu}}^K(p)$ and the integrands of Eqs. (2.22, 2.23) are periodic with respect to the Brillouin zone \mathcal{B} and analytic in a strip around the real axis. This implies locality of the perfect action.

The coupling of even and odd lattice points is due to the M_μ^K components of the fermion matrix; the M_0^K components couple even-even and odd-odd. We add without proof that even-odd decoupling of the Hermitian matrix $m^\dagger m$ can be shown in any even dimension d with arbitrary (non-degenerate) mass terms for truncated versions of the perfect fermion matrix $m(y, y')$, see Ref. [20] for $d = 2$. This is a useful property in simulations with Hybrid Monte Carlo algorithms. However, with (non-perfect) coupling to a gauge field and non-zero mass term (i.e. with even-even, odd-odd as well as even-odd couplings), this is not true in general. Yet, since even-odd decoupling of $m^\dagger m$ is a perfect property, it might be imposed as a construction requirement for a (quasi) perfectly gauged fermion vertex.

3 Optimization of Locality

In the blocking scheme described so far, there is quite some freedom left. In particular, we may use averaging functions different from Π_{BA} , and we can choose the smearing term D in Eq. (2.11). In both cases we aim at optimization of the locality in the resulting perfect action.

Let us first discuss the averaging scheme. In Eq. (2.11) we implicitly assumed the same blocking of ψ and $\bar{\psi}$, given by the weight function $\Pi(x)$ resp. its Fourier transform $\Pi(p)$. Now we consider the case of a block average $\Pi = \Pi_{BA}$ for ψ ($\bar{\psi}$) only, while $\bar{\psi}$ (ψ) is put on the lattice by decimation, $\Pi(x) = \delta(x)$. Thus we obtain a single factor $\Pi(p+2\pi l)$ in Eq. (2.14) with

$$\Pi(p) = \Pi_{BA}(p) = \prod_{\mu} \frac{\hat{p}_{\mu}}{p_{\mu}}, \quad \hat{p}_{\mu} = 2 \sin \frac{p_{\mu}}{2}. \quad (3.1)$$

In case of a δ -blockspin transformation ($D = 0$), this means to identify the averaged continuum and lattice 2-point functions

$$\langle \phi(y) \bar{\phi}(y') \rangle = \int_{[y]} dx \langle \varphi(x, H(y)) \bar{\varphi}(y', H(y')) \rangle. \quad (3.2)$$

Due to translation invariance it doesn't matter whether we average source or sink of the continuum expression, or whether we allocate the space directions to be integrated over to source and sink in some way. The last point of view may be used to make a closer contact to the construction of staggered fermions from DK fermions in the continuum [26], as discussed in Ref. [20]. We call this blocking scheme *partial decimation*. For the 2-point functions every space direction is integrated over once; therefore we do not run into the difficulties arising for blockspin transformations with complete decimation, which do not have a corresponding perfect action.

For both blocking schemes, block average for ψ and $\bar{\psi}$ (BA) and partial decimation (PD), we now want to optimize locality of the couplings by making use of the smearing terms in Eqs. (2.16, 2.17). As an optimization criterion it has been suggested to require that in the effectively 1d case – with momenta $p = (p_1, 0, \dots, 0)$ – the couplings are restricted to nearest neighbors as in the standard action [16, 18].³ In the degenerate case we require

$$i\gamma_1 M_1(p_1, 0, \dots, 0) + M_0(p_1, 0, \dots, 0) = f(m) [i\hat{p}_1 \gamma_1 + \hat{m}], \quad (3.3)$$

with $\hat{m}|_{m=0} = 0$ and $f(0) = 1$. Our ansatz for the Gaussian smearing term reads

$$D_{\mu}(p) = c(m)\hat{p}_{\mu}, \quad D_0(p) = a(m). \quad (3.4)$$

³It has been shown in Ref. [28] that this criterion does optimize locality in $d = 4$ for scalar particles over a wide range of masses.

Requirement (3.3) can be fulfilled in both blocking schemes we are considering, if we specify the RGT as follows

$$\begin{aligned} c_{BA}(m) &= [\cosh(m/2) - 1] / m^2, & a_{BA}(m) &= [\sinh(m) - m] / m^2, \\ c_{PD}(m) &= 0, & a_{PD}(m) &= [\cosh(m/2) - 1] / m. \end{aligned} \quad (3.5)$$

In both cases, we obtain $\hat{m} = 2 \sinh(m/2)$. For $m = 0$ a non-vanishing static smearing term $a(0)$ would explicitly break the remnant chiral symmetry in the fixed point action. Therefore, the static term should vanish for optimized locality, as it does in both cases. Furthermore, in the PD scheme the chiral limit is optimized for locality by a simple δ function RGT. As an advantage of this property – which is not provided by the BA scheme – there is a direct relation between the n -point functions in the continuum and on the lattice. In addition, the extension to interacting theories might involve numerical RGT steps in the classical limit, which also simplify in the absence of a Gaussian smearing term. Finally, a non-vanishing term $c(m)$ causes complications in the inclusion of a gauge interaction; the PD scheme avoids such problems.

The decay of the couplings $m(x, 0) = m(x)$ in the massless case for $d = 2$ and $d = 4$ is shown in Figures 1 and 2. We see that the PD blocking scheme works better. In

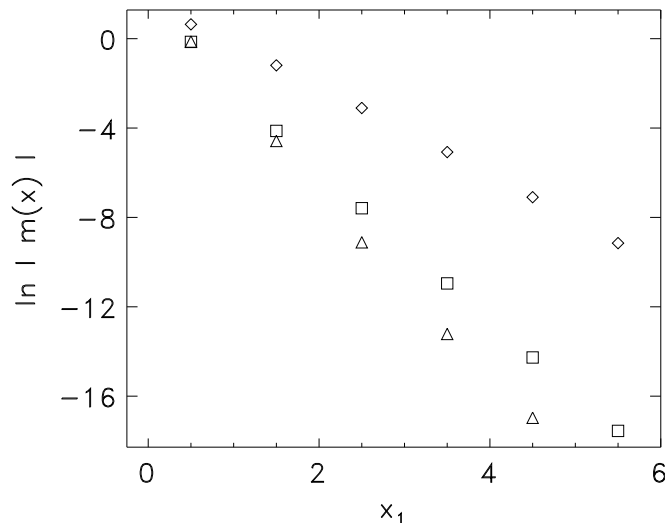


Figure 1: The decay of couplings in $(1,0)$ direction for $d = 2$ in the massless case: BA without smearing (diamonds), BA optimized (squares), PD (triangles).

the non-degenerate case the simplest ansatz for a smearing term is (corresponding to the staggered fermion action with non-degenerate mass [29])

$$D_\mu^b(p) = c \hat{p}_\mu, \quad D_0^b(p) = \sum_{K \in \mathcal{D}} \gamma_{bb}^K a_K \prod_{\mu \in K} \cos(p_\mu/2). \quad (3.6)$$

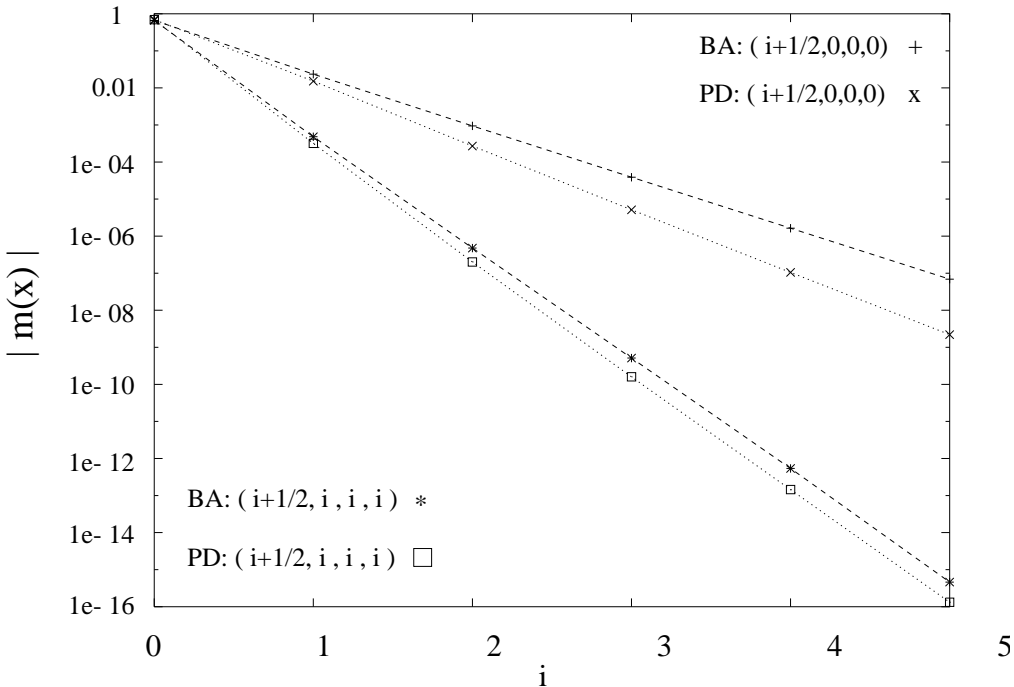


Figure 2: *The decay of 4d couplings in various directions in the massless case: BA with optimal smearing term and PD. We see that the latter decays faster.*

In this case, we obtained – by means of numerical optimization – a similar decay of couplings as with degenerate masses, yet no strict 1-dimensional ultralocality. For $d = 2$ it appears that a non-degenerate parameter $a_{12} \neq 0$ does not improve the coupling decay significantly, so we worked with $a_{12} = 0$. Again the PD scheme, where we assumed $c_{PD} = 0$, led to a more local action, see Figure 3.

4 Truncation Effects

The litmus test of any blocking scheme is given by the truncation effects for a practicable number of remaining couplings. These effects are minimized by maximal locality. Yet, the truncation scheme itself may have some impact on the truncation errors. An elegant procedure has been proposed in Ref. [22] for Wilson fermions. First the perfect action is constructed on a small lattice volume N^d by restricting the momentum components to the discrete values $p_\mu = 2\pi n_\mu/N \in]-\pi, \pi]$, $n_\mu \in \mathbb{Z}$. Typically, one chooses $N = 3$, and the resulting couplings are then used also in a large volume too, where they are not exactly perfect any more. This truncation scheme has the virtues of automatically correct normalizations, and a simplification of the numerical evaluation as opposed to a truncation in coordinate space. Furthermore, the mapping to the corresponding truncated perfect

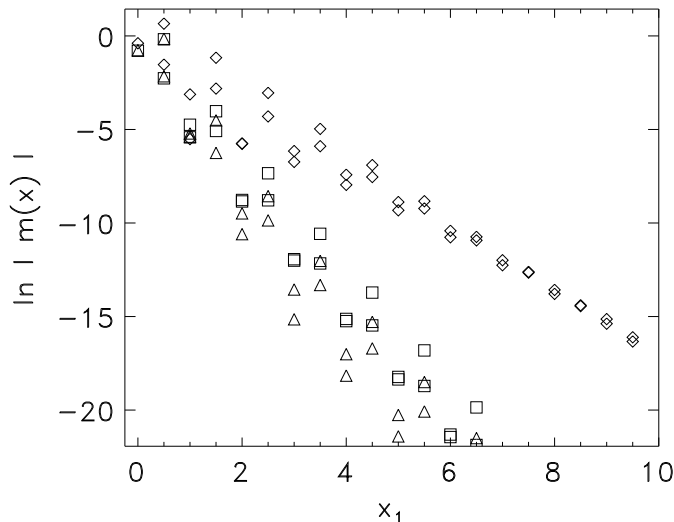


Figure 3: The decay of couplings in $(1,0)$ direction for $d = 2$ with masses $m_1=0$, $m_2=1$: BA without smearing (diamonds), BA optimized (squares), PD (triangles).

action in a lower dimension remains exact; for instance, one can reproduce the effectively 1d nearest neighbor action starting from $d > 1$ by summing over the extra dimensions, which provides a sensitive test of the numerical accuracy. Provided a good locality, this method works well for Wilson-type fermions, gauge fields [22] and scalars [28].

For staggered fermions, only a crude truncation in coordinate space has been applied so far [21]. One includes the coupling distances $\pm 1/2$, $\pm 3/2$ in the μ direction, and $1, 0, -1$ in the non- μ directions. This involves more couplings than the $N = 3$ truncated Wilson-type fermion (called “hypercube fermion”), whereas the number of degrees of freedom is the same in both cases. However, although significant improvement has been achieved compared to the standard staggered formulation, the quality of its spectral and thermodynamic properties did not reach the level of the “hypercube fermion”. In order to arrive at results of similar quality, we adapt the above truncation procedure – together with the PD scheme – to the case of staggered fermions.

We treat the components of the fermion matrix $M_{\tilde{\mu}}^K(p)$, $\tilde{\mu} = \mu, 0$ separately, as they show different behavior under reflections,

$$M_{\tilde{\mu}}^K(p_1 \dots p_{\nu-1}, -p_{\nu}, p_{\nu+1} \dots p_d) = \begin{cases} -M_{\tilde{\mu}}^K(p) & \text{for } \nu \in K\Delta\tilde{\mu} \\ M_{\tilde{\mu}}^K(p) & \text{for } \nu \notin K\Delta\tilde{\mu} \end{cases} \quad (4.1)$$

Again we use the short-hand notation $K\Delta\tilde{\mu} = K$ for $\tilde{\mu} = 0$. Truncation is achieved by discrete Fourier transformation and a discrete support given by $c_N(y_{\mu}) = 1, 1/2, 0$ for

$|2y_\mu| <, =, > N$, respectively,

$$M_{\tilde{\mu};N}^K(y) = \prod_{\mu} \frac{2\pi c_N(y_\mu)}{N} \sum_{p \in \mathcal{B}_{\tilde{\mu};N}^K} e^{-ipy} M_{\tilde{\mu}}^K(p) . \quad (4.2)$$

It is the set of discrete momenta $\mathcal{B}_{\tilde{\mu};N}^K$ which depends on the reflection properties given by $\tilde{\mu}, K$. We choose partially antiperiodic boundary conditions in y -space,

$$p \in \mathcal{B}_{\tilde{\mu};N}^K \Leftrightarrow p_\nu = \begin{cases} (2n+1)\pi/N & \text{for } \nu \in K\Delta\tilde{\mu} \\ 2n\pi/N & \text{for } \nu \notin K\Delta\tilde{\mu} \end{cases}, \quad n \in \mathbb{Z}, \quad p_\nu \in]-\pi, \pi] . \quad (4.3)$$

It is easily verified that the transformation of the truncated components back to momentum space reproduces the perfect values at $p \in \mathcal{B}_{\tilde{\mu};N}^K$,

$$M_{\tilde{\mu};N}^K(p) \equiv \sum_y e^{ipy} M_{\tilde{\mu};N}^K(y) = M_{\tilde{\mu}}^K(p) \quad \text{for } p \in \mathcal{B}_{\tilde{\mu};N}^K . \quad (4.4)$$

The components $M_{\tilde{\mu}}^K(y)$ inherit the reflection behavior of Eq. (4.1) by Fourier transformation. Therefore, treating them as periodic functions in y -space by discrete momenta $p_\nu = 2\pi n/N, n \in \mathbb{Z}$ would make them vanish at the boundaries $y_\nu = \pm N/2$ for $\nu \in K\Delta\tilde{\mu}$ artificially. We avoid this effect by the above choice of discrete momenta. It pays off by a drastic reduction of truncation effects, see Figure 4 for the 2d spectrum in the massless case using partial decimation. The values of the perfect couplings, truncated by *mixed periodic boundary conditions* as described above, are given in Table 1.

Furthermore, the truncation effects are significantly stronger for even truncation distances N ; in particular, for $N = 2$ and $N = 4$ the energies become complex-valued at large momenta.

For $N = 3$ – which we consider to be tractable in numerical simulations – the amount of improvement is already striking. We compare the spectra for $d=2$ in the PD and BA blocking scheme in the massless case (Figure 4) and for non-degenerate masses $m_1 = 0, m_2 = 1$ (Figure 5). The couplings derived from the PD blocking scheme turn out to be better, in agreement with the higher degree of locality observed in the (untruncated) perfect action. We see that the improvement is still good in the case of non-degenerate masses. In this case, we optimized the smearing parameters numerically, as discussed in Section 3. The values are $a_{BA} = 0.060, c_{BA} = 0.125, a_{PD} = 0.041, c_{PD} = 0$. The standard staggered fermion results for non-degenerate masses are calculated with the action proposed in Ref. [29]. We emphasize that the spectra of (untruncated) perfect actions are indeed perfect, i.e. identical to the continuum spectra (up to the periodicity, which is inevitable on the lattice). Hence the spectrum reveals directly the artifacts due to truncation.

Figure 6 compares the massless spectra in $d = 4$, and we see that the qualitative behavior observed in $d = 2$ persists. We compare the standard staggered fermion, and the

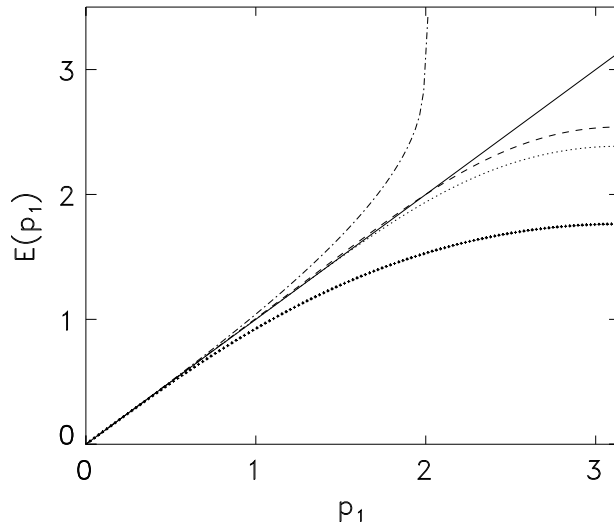


Figure 4: *The massless $d = 2$ spectrum. We compare standard staggered (fat dots) and perfect spectrum (full line) with perfect actions truncated with $N = 3$ and mixed periodic boundary conditions: block average (dotted), partial decimation (dashed). The last case is also plotted for truncation with periodic boundary conditions (dashed-dotted).*

optimized BA and PD fixed point fermions, both truncated by mixed periodic boundary conditions. We see again that the PD scheme is superior. Furthermore, we show for comparison also the dispersion relation of a Symanzik improved action called “p6” from Ref. [8]. Symanzik improvement by additional couplings along the axes (Naik fermion, [7]) only yields a moderate quality [21], but the Bielefeld group suggests a number of actions, where Symanzik improvement is achieved by diagonal couplings. The p6 action is the best variant among them, and also Figure 6 confirms its excellent level of improvement. However, it is not obvious how this formulation can include a general mass term in a subtle way.

As a further test in $d = 4$, we consider the thermodynamic ratio P/T^4 (P : pressure, T : temperature). According to the Stefan-Boltzmann law, this ratio is $7\pi^2/180$ for massless fermions in the continuum, and a lattice action with many discrete points N_t in the temporal direction will asymptotically reproduce that value. However, the speed of convergence, and in particular the behavior at small N_t , depend on the quality of the action. In contrast to the spectrum, this ratio is not even exact for the fixed point action in Eqs. (2.18, 2.19), because of the “constant factors” that we ignored when performing the functional integral in the RGT Eq. (2.11). Such factors may depend on the temperature, so with respect to thermodynamics our action is not fully renormalized [22]. However, it turns out that the unknown factor is very close to 1, except for the regime of very small N_t (about $N_t \leq 3$), which corresponds to extremely high temperature. So the main issue

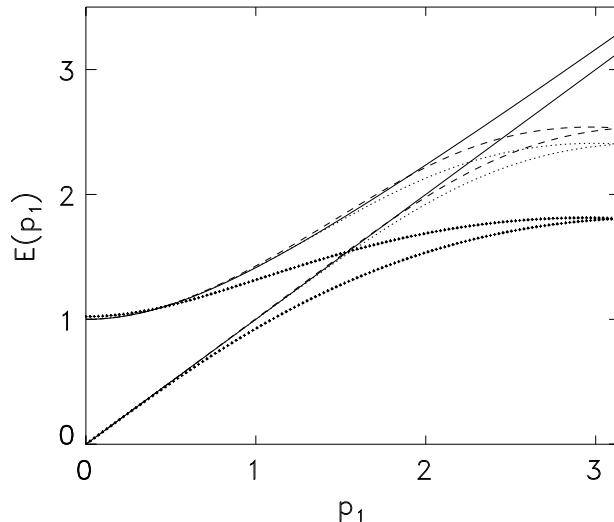


Figure 5: The $d = 2$ spectrum for $m_1 = 0, m_2 = 1$. Standard staggered (fat dots) and perfect spectrum (full line) compared with perfect actions truncated with $N = 3$ and mixed periodic boundary conditions: block average (dotted), partial decimation (dashed).

is again the contamination due to the truncation.

In Figure 7 we compare this thermodynamic scaling for a variety of staggered fermion actions at $m = 0$, and again the PD scheme turns out to be very successful. A similar level of improvement can be observed for the p6 action, which is also here by far better than the Naik fermion. We conclude that a good improvement method should in any case include diagonal couplings, which are far more promising than additional couplings on the axes (just consider rotational invariance, for example). Thus we can expand the range, in which a practically accurate continuum behavior is observed, by about a factor of 4 compared to standard staggered fermions (see Figures 4, 5, 6 and 7).

5 Conclusions

Spectral and thermodynamic results for truncated perfect staggered fermions have been presented before [21], but the improvement did not really reach a satisfactory level there. We could now push that improvement significantly further, mainly thanks to the new blocking scheme, which we call *partial decimation*, but also with the help of a new truncation technique (*mixed periodic* boundary conditions). We now reached a level of excellent improvement, similar to the results for truncated perfect Wilson-type fermions.

As a novelty, we extended the construction of perfect actions to non-degenerate flavors, and we could preserve the same level of improvement after truncation also in that case.

$d = 4$			$d = 2$		
	PD	BA		PD	BA
(0.5,0,0,0)	0.696388	0.663116	(0.5,0)	0.878234	0.866299
(0.5,1,0,0)	0.040981	0.045925	(0.5,1)	0.060883	0.066850
(0.5,1,1,0)	0.004481	0.004871			
(0.5,1,1,1)	0.000495	0.000361			
(1.5,0,0,0)	0.015219	0.023441	(1.5,0)	0.010425	0.016043
(1.5,1,0,0)	-0.000431	-0.000639	(0.5,1)	-0.005212	-0.008022
(1.5,1,1,0)	-0.000767	-0.001211			
(1.5,1,1,1)	-0.000428	-0.000635			

Table 1: The couplings of the perfect action for massless staggered fermions, constructed from the “partial decimation” (most successful) and from the optimized “block average” scheme, and truncated by mixed periodic boundary conditions. The couplings are odd in the half-integer component, and even in all other components. Among the latter there is also permutation symmetry.

This is potentially important for the study of the decoupling of heavy flavors, or for QCD simulations with realistic quark masses.

At $m = 0$, which is well described by staggered fermions, the PD scheme is optimally local if we just use a δ function RGT. This simplifies the relation to the continuum n -point functions, and numerical RGT steps, which could be performed for interacting theories (in the classical limit).

The next step is the inclusion of gauge interactions, which is not straightforward. However, also with this respect the absence of a Gaussian smearing term in the chiral limit is of advantage, because a momentum dependent smearing term – as present for the block average scheme – causes complications in that step.

As a simple ansatz, one can insert standard link variables, connect the coupled sites over the shortest lattice paths and take the mean value over these paths. This method is a simplification, which is not perfect, but for Wilson type fermions it leads for instance to a drastically improved mesonic dispersion relation [22]. In that framework, applications to the charmonium spectrum [30], pionic systems [23], and the suitable generalization of preconditioning techniques for the fermion matrix [31] are under investigation.

We have implemented this method for truncated perfect staggered fermions in $d = 2$. Including also “fat links”, we obtained promising results for the scaling properties in the Schwinger model [24] down to small inverse couplings, $\beta \leq 1$. In particular, the “pion mass” is drastically reduced compared to the staggered standard action, and the “eta mass” follows the prediction by asymptotic scaling very closely.

Acknowledgment We thank S. Chandrasekharan for his assistance.

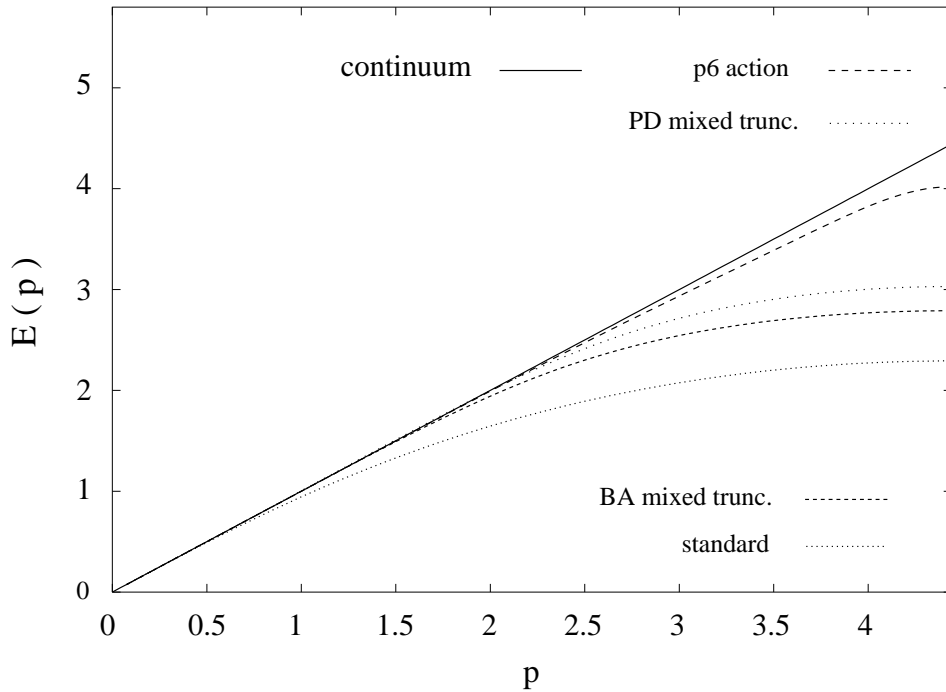


Figure 6: *The dispersion relation for various types of 4d massless staggered fermions along (1,1,0). We compare the standard action, a Symanzik improved action called “p6” from Ref. [8], and the optimized BA and PD fixed point actions, truncated with mixed periodic boundary conditions.*

References

- [1] K. Wilson *in* “New Phenomena in Subnuclear Physics” ed. A. Zichichi, Plenum, New York (1975), part A, p. 69.
- [2] L. Susskind, Phys. Rev. D16 (1977) 3031.
- [3] Proceedings of LATTICE ’97, Nucl. Phys. B (Proc. Suppl.) 63 (1998).
- [4] K. Symanzik, Nucl. Phys. B226 (1983) 187; 205.
- [5] B. Sheikholeslami and R. Wohlert, Nucl. Phys. B259 (1985) 572.
- [6] M. Lüscher, S. Sint, R. Sommer, P. Weisz and U. Wolff, Nucl. Phys. B491 (1997) 323.
- [7] S. Naik, Nucl. Phys. B316 (1989) 238.
- [8] A. Peikert, B. Beinlich, A. Bicker, F. Karsch and E. Laermann, Nucl. Phys. B (Proc. Suppl.) 63 (1998) 895.

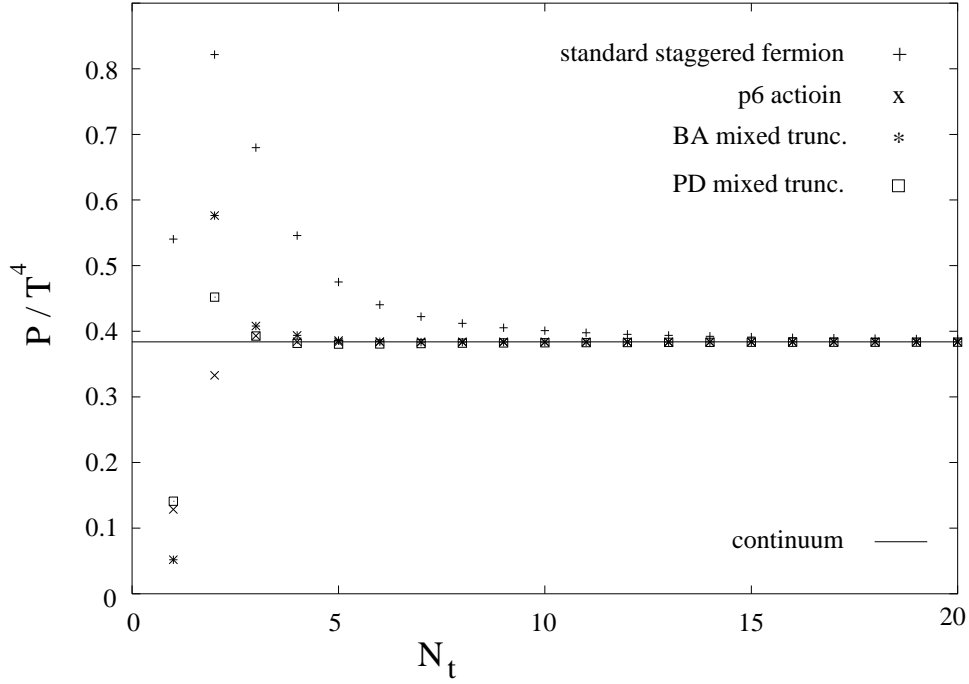


Figure 7: *The Stefan-Boltzmann law for standard staggered fermions and for the “p6 action”, compared to the truncated perfect fermions for the optimized BA and PD scheme.*

- [9] T. Blum et al., Phys. Rev. D55 (1997) 1133.
C. Bernard et al., hep-lat/9712010.
See also J.-F. Lagaë and D. Sinclair, Nucl. Phys. B (Proc. Suppl.) 63 (1998) 892.
- [10] A. Patel and S. Sharpe, Nucl. Phys. B395 (1993) 701; B 417 (1994) 307.
Y. Luo, Phys. Rev. D55 (1997) 353; Phys. Rev. D57 (1998) 265.
- [11] K. Wilson and J. Kogut, Phys. Rep. C12 (1974) 75.
K. Wilson, Rev. Mod. Phys. 47 (1975) 773.
- [12] P. Hasenfratz and F. Niedermayer, Nucl. Phys. B414 (1994) 785.
- [13] W. Bietenholz, E. Focht and U.-J. Wiese, Nucl. Phys. B436 (1995) 385.
- [14] M. Blatter, R. Burkhalter, P. Hasenfratz and F. Niedermayer, Phys. Rev. D53 (1996) 923.
M. D’Elia, F. Farchioni and A. Papa, Phys. Rev. D55 (1997) 2274.
R. Burkhalter, Phys. Rev. D54 (1996) 4121.
C. Lang and T. Pany, hep-lat/9707024.

- [15] W. Bietenholz and U.-J. Wiese, Phys. Lett. B378 (1996) 222.
F. Farchioni and V. Laliena, hep-lat/9709040.
- [16] W. Bietenholz and U.-J. Wiese, Nucl. Phys. B464 (1996) 319.
- [17] T. Kalkreuter, G. Mack and M. Speh, Int. J. Mod. Phys. C3 (1992) 121.
- [18] W. Bietenholz and U.-J. Wiese, Nucl. Phys. B (Proc. Suppl.) 34 (1994) 516.
- [19] G. Mai, “Ein Blockspin für $2^{d/2}$ Fermionen”, diploma thesis, Hamburg (1989).
T. Kalkreuter, G. Mack, G. Palma and M. Speh, *in* “Lecture Notes in Physics” 409,
eds. H. Gausterer and C. Lang, Springer, Berlin (1992) p. 205.
- [20] H. Dilger, Nucl. Phys. B490 (1997) 331.
- [21] W. Bietenholz, R. Brower, S. Chandrasekharan and U.-J. Wiese, Nucl. Phys. B 495
(1997) 285.
- [22] W. Bietenholz, R. Brower, S. Chandrasekharan and U.-J. Wiese, Nucl. Phys. B (Proc.
Suppl.) 53 (1997) 921.
- [23] T. DeGrand, hep-lat/9802012.
- [24] W. Bietenholz and H. Dilger, in preparation.
- [25] E. Kähler, Rend. Mat. Ser. V, 21 (1962) 425.
- [26] P. Becher and H. Joos, Z. Phys. C15 (1982) 343.
- [27] M. Göckeler and H. Joos, *in* “Progress in Gauge Field Theory”, eds. G. 't Hooft et
al., Plenum, New York (1984), p. 247.
M. Golterman and J. Smit, Nucl. Phys. B 278 (1986) 417.
G. Kilcup and S. Sharpe, Nucl. Phys. B 283 (1987) 493.
- [28] W. Bietenholz, Nucl. Phys. B (Proc. Suppl.) 63 (1998) 901.
- [29] M. Göckeler, Phys. Lett. B142 (1984) 197.
M. Golterman and J. Smit, Nucl. Phys. B245 (1984) 61.
- [30] K. Orginos et al., Nucl. Phys. B (Proc. Suppl.) 63 (1998) 904.
- [31] N. Eicker et al., Nucl. Phys. B (Proc. Suppl.) 63 (1998) 955; and in preparation.